Scaling of structure and electrical properties in ultra-thin epitaxial ferroelectric heterostructures.

V. Nagarajan[1*], J. Junquera[2*], J. Q. He[3], C. L. Jia[3], K. Lee[4], Y. K. Kim[4], T. Zhao[5], Ph. Ghosez[6], K. M. Rabe[7], S. Baik[4], R. Waser[3] and R. Ramesh[5]

1. School of Materials Science and Engineering, University of New South Wales, Sydney NSW, AUSTRALIA

2. Department of Physics, University of Cantabria, Santander, SPAIN.

3. Centre of Nanoelectronic Systems for Information Technology, Dept IFF, Forschungszentrum Juelich, D52425 GERMANY

4. Department of Materials Science and Engineering, Pohang University of Science and Technology, Pohang 790-784, KOREA.

5. Dept of Materials Science and Dept of Physics, University of California, Berkeley, CA 94720

6. Universite de Liege, Institut de Physique, Bat. B5, Allee du 6 aout, 17 B- 4000 Sart Tilman BELGIUM

7. Dept. of Physics and Astronomy, Rutgers University, Piscataway, New Jersey 08854–8019, USA.

[*] These authors contributed equally to this work.

Abstract

Scaling of the structural order parameter and the polarization was investigated in model ultra-thin epitaxial $SrRuO_3/PbZr_{0.2}Ti_{0.8}O_3/SrRuO_3/SrTiO_3$ heterostructures. High resolution transmission electron microscopy images revealed the interfaces to be sharp and fully coherent. Synchrotron x-ray studies show that a high tetragonality (c/a~1.058) is maintained down to 50 Å thick films, suggesting indirectly that ferroelectricity is fully preserved at such small thicknesses. However, measurement of the switchable polarization (ΔP) using a pulsed probe setup and the out-of-plane piezoelectric response (d_{33}) revealed a systematic drop from ~140 $\mu C/cm^2$ and 60 pm/V for a 150 Å thick film to 11 $\mu C/cm^2$ and 7 pm/V for a 50Å thick film. This apparent contradiction between the structural measurements and the measured switchable polarization is explained by an increasing presence of a strong depolarization field, which creates a pinned 180° polydomain state for the thinnest films. Existence of a polydomain state is demonstrated by piezoresponse force microscopy images of the ultra-thin films. These results suggest that the limit for a ferroelectric memory device may be much larger than the fundamental limit for ferroelectricity.

INTRODUCTION

The reorientable electric polarization of ferroelectric materials has long been of interest for its potential in high density information storage. [1,2] One of the most crucial questions regarding the densities and performance that can ultimately be achieved is that of the size effect [3,4] on the magnitude and stability of uniform switchable polarization. In the past few years, careful measurements on high-quality ultra-thin films[5-13] and related theoretical models [14-17]for thin films have shown that a ferroelectric instability can be exhibited by perovskite oxide films as thin as a few lattice constants. This has led to renewed interest in understanding the scaling of ferroelectric properties with thickness in the ultra thin regime. To preserve states with uniform polarization, the compensation of the depolarization field has been identified as a crucial factor [17-20] On $SrTiO_3$ (STO) insulating substrates, x-ray studies of films of $PbTiO_3$ (PTO) exhibit a polar distortion, but to reduce depolarization energy the system forms periodic 180° ferroelectric stripe domains.[10] Metallic electrodes under short-circuit conditions should provide a mechanism for compensation of the depolarization field that acts to stabilize the uniformly polarized state. However, in real conductors the screening is imperfect. As the films get thinner, the residual field in the ferroelectric due to the surface-dipole density at the ferroelectric/electrode interface grows [17,19] resulting in renormalization of the coercive field [21], reduction in polarization of uniformly polarized films [22] and ultimately a possible destabilization of ferroelectricity in the thinnest films.

For information storage technology, the figure of merit is the magnitude and stability of the switchable ferroelectric polarization. This is referred to as ΔP and ideally is twice the remnant polarization. Measurements of the thickness variation of the

magnitude of ΔP for uniformly polarized films in the sub-100 Å thickness regime are therefore of particular interest, as this magnitude is expected to be modified by the residual depolarizing field and other corrections resulting from the imperfect screening in the electrodes. Recently Noh et al showed ferroelectric hysteresis loops for epitaxial $BaTiO_3$ (BTO) films as thin as 50 Å .[13] Structurally they observe that even the 50Å film exhibits c-axis value that is considerably larger than the bulk values for BTO while the polarization for the 50Å film is considerably lower than the bulk value for BTO. They see a systematic reduction in the polarization as a function of reducing thickness, and their experimental data agrees well with the theoretical first principles based predictions of Ghosez and Junquera.[17] In contrast a systematic study of PTO ultra-thin epitaxial films by Triscone et al showed a monotonic decrease in the lattice tetragonality with decreasing thickness.[22] Further for certain ferroelectrics a clear resistance switching effect was observed when scaled to very low thickness.[23,24] There is also theoretical understanding now that predicts tunneling effects in ultra-thin ferroelectric barriers sandwiched between metal electrodes.[25] Thus there exists still a conundrum, particularly in epitaxial ultra-thin heterostructures, as to how the lattice and polarization properties scale with thickness for different ferroelectric compositions.

To understand this we combined direct measurements of the switchable ferroelectric polarization and piezoelectric responses with information about the structure to study scaling effects in a model heterostructure system of high quality ultra-thin $PbZr_{0.2}Ti_{0.8}O_3$ (PZT) films with $SrRuO_3$ (SRO) electrodes. The thinnest films show a sharp drop in the measured ΔP and the out-of-plane piezoelectric constant but virtually no change in the lattice constants. This observation is successfully explained by the

depolarization field model, in which decreasing thickness leads to increases in the residual field that destabilize the system into a 180˚ domain state similar to that observed on an insulating substrate.[10,20]

II. Experiment

Epitaxial PZT ultra-thin films from 50 to 500 Å thick were grown on SRO buffered (100) STO substrate by pulsed laser deposition. Details of the growth are given elsewhere.[12] The maximum thickness of the PZT film presented in this study was limited to 500 Å, in order to maintain fully c-axis oriented films and avoid the formation of ferroelastic a-axis domains. (90°-domains). The microstructure and local distortion in ultra-thin films was investigated by means of high-resolution transmission electron microscopy (HRTEM). HRTEM images were obtained using a JEOL-4000EX high-resolution electron microscope operating at 400 keV with point to point resolution of 0.17 nm.
Lattice constants for films greater than 500Å thickness were measured using a conventional X-ray diffractometer fitted with thin film optics. The lattice parameters for the 50Å and 80Å PZT films were investigated by synchrotron x-ray diffraction at the Pohang Light Source (PLS). The beam size at the focal point is typically less than 1 mm^2. A scintillation detector was used to record the diffracted beam intensities.

To ascertain that the ultra-thin films have low leakage paths, direct current-atomic force microscopy (DC-AFM) was used to image leakage current paths of these ultra-thin films. The images were obtained at room temperature and under 10^{-3} Bar on a JEOL STM/AFM with 1pA detection limit. This technique has been used to image dislocations in semiconductors [26], leakage in SiO_2 MOS structures[27], nanoscale current transport[28] and screening phenomena in oxide ferroelectrics[29]. Basically in this technique

a voltage is applied between a conducting tip and the sample and the resulting current is detected using a current pre-amplifier / I-V converter. The current images are obtained simultaneously with topography and hence allow the correlation of electrical properties with topological features.

Direct quantitative ferroelectric properties were evaluated using a pulse method using an atomic force microscope (AFM). [30] This technique facilitates measurement of nanoscale sub-micron capacitors and with fast rise times, both very important to successfully test ferroelectric nanostructures. The pulsed probe method was chosen over the traditional P-E hysteresis measurement as it is less convoluted by leakage and non-linear dielectric effects. However to check the existence of resistive switching effects, the thinnest film was swept under a voltage bias as would be for a hysteresis measurement. To avoid leakage paths sub-micron sized capacitors were created, especially for the thinnest film, using a modified lift off process. The typical lateral area of the capacitors for the 50Å film was 0.125 μm^2 while for the thicker films were 4 μm^2.Quantitative piezoresponse force microscopy (PFM) [31] was used to measure the piezoelectric (d_{33}) responses. The deflection of the PFM tip was calibrated using a X-cut quartz crystal. Further details on the PFM calibration can be found in ref [32] .[32]

III. Results and Discussion

(A) STRUCTURAL MEASUREMENTS:

Figure 1(a) is a cross sectional HRTEM image of a PZT/SRO/STO heterostructure,[*] with the PZT of nominal thickness 50 Å. In our previous report we presented cross-sectional HRTEM data on a film that was 40 Å thick.[12] In that case, the average lattice

---

[*] The presence of a top SRO hindered the resolution of the TEM image. For all electrical and piezoelectric measurements a top SRO/Pt electrode was used.

tetragonality (*c/a* ratio) was calculated based on the power spectrum of a lattice image to be 1.05. In the present report we show a detailed analysis of the local lattice strain of the film by lattice mapping directly on the image using a numerical center-of-mass approach. In the image of fig. 1(a) the distance between the top free surface (dashed line) and the bottom ferroelectric-electrode interface (arrow) is approximately 14 layers, each a single unit cell thick. In fig 1(b) we plot the measured *c* and *a* axis parameter and in fig 1(c) we plot the *c/a* ratio as a function of each layer. All parameters were calibrated with respect to lattice parameter of the STO substrate, which was fixed at 3.905 Å. We find two key observations. Firstly a slight decrease in the out-of-plane parameter and hence the tetragonality is observed at the interfaces compared to the interior of the PZT layers; the exact reasons for this are unclear. Recently Tybell and co-workers used low-angle annular dark-field (ADF) scanning transmission electron microscopy to show that epitaxial $PbTiO_3/SrTiO_3$ (PTO/STO) films display a strained interface.[33]. They too found that careful comparison between the lattice parameters in the volume of the thin films to the interface unveiled a reduced *c*-axis lattice parameter near the film/substrate interface. This trend may be compatible with the scenario of an extrapolated length [14,16] for thin films, where in surface effects induce a suppression of the polarization and hence lattice parameter.

Secondly the measured *c*/*a* ratio (ranging from 1.07 to ~1.09) from the high-resolution image is higher than those reported by x-ray (as discussed in the next section) for this PZT composition. It is difficult to convolute if the high tetragonality is an intrinsic effect or due to, for example, thin foil effects, residual strain, or electron beam irradiation effects. We point out that Stemmer *et al* [34] obtained a tetragonality of 1.09 near domain

walls in $PbTiO_3$ thin films by direct analysis of HRTEM images, which is higher than the expected value of 1.06. There is no satisfactory quantitative explanation of this difference; thus the only inference from the HRTEM images is that the lattice is highly tetragonal.

Due to the above inherent issues with HRTEM analysis we further probed the structural parameters via X-ray diffraction. Fig 2(a) is a theta-2theta scan of the 50Å sample using Synchrotron source at PLS. The (001) PZT, (100) SRO and (100) STO peaks are indicated on the graph. Again the lattice parameter of the STO substrate was used to calibrate the peak positions. From this graph we measure the out-of-plane lattice parameter to be 4.132Å. To measure the in-plane scan the sample was tilted to obtain diffraction from the (102) reflection. This is shown in figure 2(b). The in-plane lattice parameter was calculated to be 3.905Å and hence the tetragonality of the 50 Å film is ~1.058. Similar scans were performed for each of the thickness in the series. Fig 2(c) is a graph of the tetragonality measured as a function of the film thickness. It demonstrates that for films less than 200 Å thick there is ~1% increase in tetragonality compared to the bulk c/a of 1.05, indicating the films are compressively stressed in-plane; above this thickness the tetragonality relaxes by dislocation formation. Although there is some difference between the HRTEM and X-Ray measurements, the overall conclusion is that a high tetragonality is maintained down to 50Å thickness. A similar trend was observed for BTO ultra-thin films in the report by Noh et al.[13]. For films thinner than 350Å and down to 50Å a strong increase in the c lattice parameter compared to bulk BTO (an elongation of 6%) was observed, indicating a residual compressive strain in the plane of

the substrate. For films thicker than 350Å the out-of-plane parameter relaxed to bulk like values - this was attributed to relaxation by misfit dislocations.

Due to the strong polarization-strain coupling [35] in PTO rich systems a high tetragonality is associated with a high polarization. Thus the trend shown by the c/a ratio as a function of thickness suggests that even below sub-100Å thickness range, a large value of the polarization is sustained.

(B) ELECTRICAL MEASUREMENTS:

To ensure that the ultra-thin films were of high quality we performed DC AFM images to identify potential sources of leakage or breakdown. Here we show results from scans performed on the 50Å thick film. Fig 3(a)-(d) is a set of typical 1x 1 μm^2 images (more than twice the area of the test capacitor devices) obtained for a 50Å PZT grown on SRO/STO. The legend on the right to each image shows the current passing through the sample. We see that up to 0.8V (~1.6 MV/cm) there is a uniform contrast indicating the lack of high conduction paths although the total current shows a slight increase. Only when the applied voltage is 1.5 V (3 MV/cm) does the sample show break down, as indicated by the large number of white/light colored regions in the image. Therefore we concluded that even the thinnest films were able to withstand local electric fields almost as high as 3 MV/cm.

Fig 4(a) shows a set of switching transients recorded by the PUND method measured at 2.5 MV/cm and 2 μsec pulse width for 4 typical thicknesses: 300, 150, 120 and 80 Å. The inset to fig 4(a) shows the transients for the 50 Å thick film. No resistance switching were observed for the ultra-thin film, unlike reports on $PbZr_{0.52}Ti_{0.48}O_3$ ultra-thin films[23] Fig 4(a) shows a clear decrease in the magnitude as a function of decreasing thickness.

Each switching transient was integrated to obtain the measured ΔP. To ensure mathematical rigor we used the "double deflection" method, [30] In figure 4(b) we show the results of the integration for each thickness. Films 150 Å and thicker show a ΔP of ~150 μC/cm^2. Below 150Å, it progressively decreases to approximately 11 μC/cm2 for the 50Å film. Thus the polarization measurements reveal a systematic reduction in ΔP as a function of decreasing film thickness, i.e., a size effect as the thickness is scaled down. This again is very similar to the trend shown by BTO ultra-thin films; very high tetragonality coupled with vanishing switched polarization. [13] However no comment was made for this contrasting trend. Further fig 4(c) plots the switched polarization as a function of applied field for each thickness. It is observed that films thicker than 150Å saturate to high switched polarization values; on the other hand the ultra-thin films show no indications of saturation. Beyond these values of applied electric field significant breakdown was observed; hence convoluting the observed response. It is thus concluded that the ultra-thin films show a highly pinned behavior and are unable to reach fully switched polarization even at extremely large electrical fields.

In figure 5 the out-of-plane piezoelectric response (d_{33}) is plotted as a function of thickness. The presence of a top electrode ensured a uniform distribution of the electric field. Figure 5 (a) is a set of d_{33} loops for 5 different thicknesses, from 4 nm to 30 nm. With decreasing film thickness, the piezoresponse decreases in a systematic and smooth manner. The piezoresponse is 60 pm/V for the 30 nm film which drops to only 7 pm/V for the 4 nm thick film. Fig 5 (b) plots this drop. The error bars are standard deviations of the measurements. A striking resemblance is seen for the d_{33} thickness dependence vis-à-vis the polarization thickness dependence. This trend is not expected in the event of a real

size driven phase transition; the piezoelectric response is expected to diverge with decreasing thickness in the case of a real size effect. [36-38] Secondly with decreasing thickness, a systematic increase in the coercive field is observed, in compliance with previous reports. It increases from 150 kV/cm for the 30 nm thick film to 1300 kV/cm for the 8 nm film. The reason for this increase is still under debate; explanations range from cross-over from nucleation and growth of domains to intrinsic switching [5] to the presence of a strong depolarizing field which must be corrected for.[21] Also with decreasing thickness the electric field dependence of the d_{33} progressively decreases while the tilt of the loop increases. The reason for this increasing tilt is attributed to the presence of passive layers as demonstrated by Tagantsev et al in a series of papers.[39,40] We have performed a detailed analysis of the tilting of the loop based on the approach of Tagantsev et al. In this article we purposely avoid discussing it in detail as it forms a more detailed study in itself. [41] Thus both the polarization and piezoelectric properties are in direct contradiction to our structural data, which show negligible size effects in the tetragonality.

The most important features of the above experimental observations are as follows:

(i) An enhancement of tetragonality of about 1% with respect to the bulk for films thinner than 200 Å,

(ii) A lack of scaling for tetragonality with thickness in the sub 100 Å range,

(iii) A clear decrease in the magnitude of the switchable polarization with decreasing thickness, and

(iv) A substantial reduction of the out-of-plane piezoelectric response for the thinnest films.

Due to the well-known strong polarization-strain coupling in ferroelectric perovskite oxides, explicitly checked by first-principles calculations at the bulk level for PZT[†] , (i) and (ii) suggest the existence of a ferroelectric polarization in the system, whereas (iii) and (iv) point to a paraelectric ground state with no net polarization.[‡]

(C) THEORY

To resolve this apparent inconsistency, we have carried out first-principles effective Hamiltonian simulations. It could be surmised that the presence of ionic defects (e.g. oxygen vacancies) or electronic charge carriers could possible lead to elongated lattice parameters[42] or would pin domain walls[43,44] and therefore reduce the measured switchable polarization. While we cannot fully neglect the effect of oxygen vacancies, generally such ionic vacancies are expected to increase leakage currents dramatically.[45] This is not the case as shown by the DC-AFM images. Additionally XPS measurements did not show any measurable changes in the $Pb+^{2}$ or Ti^{+4}peak positions as a function of film thickness, therefore we also precluded changes in the electronic states of the cations as the major cause for the reduction in polarization.

We use the parameters for pure PTO, [46] as the main effect of the 20% Zr alloying is to only slightly shift the transition temperature and spontaneous polarization. Following a well-established precedent, the structure and properties of the thin film are obtained from simulation of the bulk material with the corresponding epitaxial strain constraint and

† First-principles density-functional calculations on bulk $Pb(Zr_{0.2}Ti_{0.8})O_3$ confirm that the polarization along the c-axis steadily grows with the increasing of the tetragonal order parameter over a wide range of c/a.

‡ A similar trend was observed as well in the report by Noh et al for epitaxial $BaTiO_3$ films; however no comment is made.

macroscopic electric field [17,22]. In the present case, the in-plane lattice vectors are fixed to match the cubic STO substrate (3.905 Å). Previous first-principles calculations[17] have shown that short circuit boundary conditions across the entire system result in a nonzero macroscopic field in the thin film that depends linearly on the polarization of the thin film, and is inversely proportional to the thickness of the ferroelectric layer. This residual depolarization field E_d couples with the polarization yielding an extra electrostatic energy that tends to suppress the polarization [19] . Only the net component of the out-of-plane polarization is considered here to compute the homogeneous depolarization field E_d and the corresponding contributions to the energy.[§]

The thickness dependence of the normal average polarization P, tetragonality c/a, and the out-of-plane piezoelectric constant (d_{33}) at room temperature, obtained by classical Monte Carlo simulations for a 12x12x12 supercell, are presented in Fig. 6. We have performed simulations as a function of cell size and confirmed that the results are independent of cell size. A sharp monodomain-polydomain phase transition, driven by E_d, is detected at a thickness around 150 Å. This is similar to phase transitions reported in Refs. [47,48]. The phase transition results from the competition between the compressive strain imposed by the substrate, which tends to stabilize the tetragonal phase [49],[50,51] and the out-of-plane polarization, and a depolarization field that tends to suppress the latter. As the film gets thinner, the residual field in the ferroelectric grows and, consequently, both the polarization [17] and the tetragonality [22] are progressively reduced (see Fig 6 (a-b)) Below the critical thickness the system breaks up into equal-width 180º stripe domains (net polarization zero) to minimize the energy associated with E_d.(Fig 7 (a-c)) This

§ The absence of the stray energy spoils the applicability of our model to thickness below the domain width (in our simulations half of a supercell, that is, around 24 Å). A more detailed model is needed for the thinnest films.

domain structure has been observed and characterized in ultra-thin PTO films grown on insulating substrates[8,10] Here, we propose its existence as the mechanism for compensation of the depolarization field for ferroelectric layers sandwiched between metallic electrodes as well. Though the net switchable polarization is zero, each domain exhibits the bulk strained polarization and tetragonality c/a, 1.25 % larger than in the unstrained sample, explaining the apparent inconsistency of the experimental data. Moreover, since the out-of-plane piezoelectric response is also directly proportional to the polarization inside each domain, its average also tends to cancel for films thinner than the threshold thickness, explaining the drop of d_{33} experimentally observed (Fig. 6 (c)). One might expect that a transition from the 180° domain state to the uniformly polarized state could be induced by the application of a sufficiently high electric field; however, experimentally this is not observed as shown by figure 4(c).

Simulations of the response of the system under high electric field were carried out to check the strong nature of the pinned domain state. In Fig. 8 we represent the results of the Monte Carlo simulations under the presence of a field of 3 MV/cm. It is seen that even under such high fields, the theoretically calculated switched polarization for the sub 100Å thick films are very small. In order to explain this behavior, it necessary to understand the different energies involved. Let us start with a 50/50 domain structure as the one described in the preceding paragraph. In such a configuration, the switchable polarization is zero. The net polarization at the surface $< P >$ also vanishes, and consequently there is no depolarization field $\mathcal{E}_d$.

$$
\begin{aligned}
&< P >= 0, \\
&\mathcal{E}_d = \frac{-2\lambda < P >}{\varepsilon_0 d} = 0,
\end{aligned}
\tag{1}
$$

where λ stands for the effective screening length of the electrode and d is the thickness of the ferroelectric thin film (we use SI units).

Now, let's switch on an external field $\mathcal{E}_{appl}$ pointing up. This field couples with the polarization inside each domain, and the corresponding electrostatic energy coupling E_{appl} will be given by

$$
\begin{aligned}
E_{appl} &= -\int_{\Omega} \mathcal{E}_{appl} P d\Omega = -\int_{\Omega_{up}} \mathcal{E}_{appl} P d\Omega_{up} - \int_{\Omega_{down}} \mathcal{E}_{appl} P d\Omega_{down} = -\mathcal{E}_{appl} P\left(\Omega_{up} - \Omega_{down}\right) \\
&= -\mathcal{E}_{appl} < P > \Omega,
\end{aligned}
\tag{2}
$$

where Ω_{up} and Ω_{down} stand for the volume of the domains up and down respectively, Ω refers to the whole volume of the sample, and we have supposed that both the local polarization (the same in magnitude inside each domain) and the applied field are homogeneous. In the previous expression, we have made use of the fact that $\mathcal{E}_{appl}$ is parallel to the polarization up and antiparallel to the polarization down. Clearly, the electrostatic energy is linear in the net polarization, the domain being down energetically favorable against domain up. That means that in the absence of a depolarization field, the system will minimize the energy by flipping all the domains down completely.

However, as soon as the domain wall is displaced, a net polarization $< P >$ appears, giving rise to a proportional depolarization field $\mathcal{E}_d$ (Eqn-1). The corresponding energy coupling E_{dep} is positive in sign (that is it tends to suppress the polarization) and quadratic on the net polarization [22,37]

$$E_{dep} = +\frac{2\lambda < P >^2}{\varepsilon_0 d} \qquad (3)$$

As seen above the depolarizing energy is inversely proportional to the thickness of the thin film, so the thinner the film, the larger the depolarizing energy for a given net polarization. The total electrostatic energy to be minimized will be given by the sum of E_{appl} and E_{dep}. The presence of the quadratic term avoids the free creeping of the domain walls, explaining why such a high field is not large enough to induce a transition to a monodomain uniformly polarized state, thereby creating pinning of the domains and hence inducing low switched polarization in good agreement with the experimentally observed trends.

In other words, an external applied field couples linearly with the local polarization inside each domain, favoring the domain with the polarization parallel to it against the other. As soon as the domain wall is displaced, a net polarization P appears, giving rise to a proportional non-vanishing depolarization field. The corresponding energy coupling is quadratic in P and positive in sign, so it drives the domain wall back to restore the 50/50 configuration, preventing the free creeping of the domains walls.

Although the above scenario can explain in general the experimental trends there are some differences between the experimentally observed size dependence behavior and the theoretical simulations. Most prominently, the theoretical simulations predict a very sharp fall in the ferroelectric properties while in the experimental data it is more gradual. This arises from a primary difference that the experimental plot is that of a switched polarization under a given applied electric field whereas the ab-initio simulations of figure 6 show the case of remnant polarization as a function of thickness. It is highlighted again, that the polarization measurements reported here were performed by the PUND

method (which necessitate application of an electric field) and not ferroelectric hysteresis loops. Indeed when the simulations are performed under an applied electric field, the drop is gradual as observed in figure 8.

Secondly the experimentally observed remnant piezoelectric response for the sub 100Å films (although only 7-15 pm/V) is not zero, where as the theoretical simulations predict a vanishing piezoresponse on account of the polydomain state. This is because the remnant state in the loop is reached only after sweeping to the maximum positive electric field, on its way to maximum negative electric field. Thus there is a history dependent path involved, which cannot be accounted for by the theoretical simulations.

To check the presence of an 180^0 polydomain state we performed piezoresponse force microscopy (PFM) imaging of the as grown samples.[**] Fig 9 compares the PFM images of 2 thicknesses-150Å and 50Å. Fig 8(a) is 5 by 5 micron PFM scan of the 150Å film. At the center a 3 by 3 micron region is switched by application of +5 V and within that a 1 by 1 micron region is switched by applying a reverse bias of -5V. Time dependent scans of the images did not reveal any decrease or relaxation of the piezoresponse, suggesting that the written regions were extremely stable.[6] Fig 9(b) is the profile along section AA' as drawn in fig 9(a). The following interesting observations can be made:

(a) Outside the written zone line scan of the virgin region is uniformly negative, which suggests that the as grown film has a uniform polarity. *In other words the 150Å thick film is monodomain.* This is in good agreement with the theoretical predictions.

[**] We performed synchrotron experiments as well to check the presence of satellite peaks as demonstrated by Fong et al. (Refs 8,10) However the Pohang beam line does not have adequate beam energy to resolve the peaks. Therefore we retorted to the technique of PFM.

(b) Application of the positive bias (region marked with "+") creates regions of opposite contrast and changes the sign of the piezoresponse signal (as seen in fig 9 (b)) to positive but the magnitude is approximately the same demonstrating that regions can be fully switched. This is in good agreement with the quantitative piezoelectric and the polarization measurements discussed earlier.

(c) Application of negative bias (region marked as "-") reverts the piezoresponse and hence the polarization back to the original contrast.

Fig 9(c) is the PFM scan for the 50Å thick film with identically repeated write experiments. Fig 9 (d) plots the profile for line BB' in fig 9(c). It is found that in comparison to the 150Å sample images, the result for the 50 Å film is significantly different in the following manner:

(a) Most importantly the virgin surface shows a piezoresponse very close to zero. In fig 9(d) this is the region inside the circle. This indicates that film has a polydomain state such that the response is approximately zero.

(b) On application of the positive bias, there is piezoresponse signal and the magnitude is positive. In this state all dipoles are pointed towards the bottom electrode. This indicates the film can be switched however the magnitude of the written region is less than 20% of the 150Å region, in agreement with the trend shown by quantitative PFM.

(c) On applying the reverse negative bias, it is observed that central region ("-") does not switch back to a negative state but in fact hovers around zero, i.e., returns to the virgin state. This implies that the pinned polydomain state is stable favored to a uniformly negative monodomain state. This is slightly different from our

quantitative results, where in a piezoresponse is observed, similar in magnitude to the positive cycle. This difference may arise from the asymmetry of electrodes used in imaging experiments.

We thus conclude that the PFM studies indicate that the sub 100 Å ultra-thin film is polydomain thereby validating the conclusions of our theoretical simulations.

IV. CONCLUSIONS

In summary, we show in ultra-thin SRO/PZT/SRO heterostructures a strikingly anomalous behavior; virtually no scaling of the tetragonality down to 50Å thickness accompanied by a systematic reduction of the switchable polarization and the out-of-plane piezoelectric constant. First principles simulations predict the formation of an 180° polydomain state for the thinnest films due to the presence of a residual depolarization field. The presence of a polydomain state is experimentally indicated by PFM images. Both the simulations and experiments suggest that this polydomain state is pinned and therefore explain the observed anomaly. Our studies on epitaxial perovskite ferroelectric thin films therefore indicate that although ferroelectricity is maintained down to nanometer level thickness, switchable polarization is severely affected.

It is also pertinent here to ask why polarization saturation cannot be observed in our films where as no size effects and complete saturation was reported for ultra-thin PVDF polymer films.[5] The reason for this may perhaps be that the nature of ferroelectricity in PVDF is different compared to PZT; this is a topic of our current investigation. Furthermore why resistance switching is not observed for this composition while it is seen for other PZT compositions needs further investigations.

Acknowledgements:

This work was supported by NSF MRSEC grant DMR 00-80008 and a NSF US-DFG collaborative grant No. DMR 02-44288. The work at Liege and Juelich was supported by the VolkswagenStiftung (1/77 737). Ph. G also acknowledges the support of FNRS-Belgium (contract 2.4562.03) and the European Network of Excellence "FAME" (contract FP6-500156-1). V. N acknowledges the Alexander von Humboldt foundation for his stay in FZ-Juelich, Germany. We acknowledge helpful discussions with Dr. H.H. Kohlstedt and Dr. Dawber and the help of Prof. Szot for the DC-AFM images.

References:

[1] J. F. Scott and C. A. P. de Araujo, Science 246, 1400 (1989).

[2] R. Waser, *Nanoelectronics and Information Technology* (Wiley-VCH, 2003).

[3] T. M. Shaw, S.-T. McKinstry, and P. C. McIntyre, Ann. Rev. Mat. Sci 30, 263-298 (2000).

[4] C. H. Ahn, K. M. Rabe, and J.-M. Triscone, Science 303 (2004).

[5] A. V. Bune, V. M. Fridkin, S. Ducharme, L. M. Blinov, S. P. Palto, A. V. Sorokin, S. G. Yudin, and A. Zlatkin, Nature 391, 874 - 877 (1998).

[6] T. Tybell, C. H. Ahn, and J.-M. Triscone, Appl. Phys. Lett. 75, 856-858 (1999).

[7] N. Yanase, K. Abe, N. Fukushima, and T. Kawakubo, Jpn. J. Appl. Phys 38, 5305-5308 (1999).

[8] S. K. Streiffer, J. A. Eastman, D. D. Fong, C. Thompson, A. Munkholm, M. V. R. Murty, O. Auciello, G. R. Bai, and G. B. Stephenson, Phys. Rev. Lett. 89, 67601-604 (2002).

[9] M.-W. Chu, I. Szafraniak, R. Scholz, C. Harnagea, D. Hesse, M. Alexe, and U. Gösele, Nature-Materials 3, 87-89 (2004).

[10] D. D. Fong, G. B. Stephenson, S. K. Streiffer, J. A. Eastman, O. Auciello, P. H. Fuoss, and C. Thompson, Science 304, 1651 (2004).

[11] H. Ishiwara, M. Okuyama, and Y. Arimoto, *Ferroelectric Random Access Memories: Fundamentals and Applications*, Vol. 93 (Springer-Verlag, 2004).

[12] V. Nagarajan, T. Zhao, J. Ouyang, R. Ramesh, W. Tian, X. Q. Pan, D. M. Kim, C. B. Eom, H. Kohlstedt, and R. Waser, Appl. Phys. Lett. 84, 5225-5227 (2004).

[13] Y. S. Kim, D. H. Kim, J. D. Kim, Y. J. Chang, T. W. Noh, J. H. Kong, K. Char, Y. D. Park, S. D. Bu, J. G. Yoon, and J. S. Chung, Appl. Phys. Lett. 86, 102907 (2005).

[14] R. Kretschmer and K. Binder, Phys. Rev. B 20, 1065-1076 (1979).

[15] P. Ghosez and K. M. Rabe, Appl. Phys. Lett. 76, 2767-69 (2000).

[16] A. G. Zembilgotov, N. A. Pertsev, H. Kohlstedt, and R. Waser, J. App. Phys. 91, 2247-2254 (2002).

[17] J. Junquera and P. Ghosez, Nature 422, 506-509 (2003).

[18] M. D. Glinchuk, E. A. Eliseev, and V. A. Stephanovich, Physica B 322, 356-370 (2002).

[19] I. P. Batra, P. Wurfel, and B. D. Silverman, J. Vac. Sci Technol 10, 687-692 (1973).

[20] Z. Q. Wu, N. D. Huang, Z. R. Liu, J. Wu, W. H. Duan, B. L. Gu, and X. W. Zhang, Phys. Rev. B 70 (2004).

[21] M. Dawber, P. Chandra, P. B. Littlewood, and J. F. Scott, J. Phys.: Condens. Matter 15, L393–L398 (2003).

[22] C. Lichtensteiger, J.-M. Triscone, J. Junquera, and P. Ghosez, Phy. Rev. Lett. 94, 047603-1 (2005).

[23] J. R. Contreras, H. Kohlstedt, U. Poppe, C. Buchal, N. A. Pertsev, and R. Waser, Appl. Phys. Lett. 83, 495-497 (2003).

[24] H. Qu, W. Yao, T. Garcia, J. Zhang, A. V. Sorokin, S. Ducharme, P. A. Dowben, and V. M. Fridkin, Appl. Phys. Lett. 82, 4322 (2003).

[25] M. Y. Zhuravlev, R. F. Sabirianov, S. S. Jaswal, and E. Y. Tsymbal, Phys. Rev. Lett. 94, 246802 (2005).

[26] B. S. Simpkins, E. T. Yu, P. Waltereit, and J. S. Speck, J. Appl. Phys. 94, 1448-1453 (2003).

[27] M. Porti, M. Nafria, X. Aymerich, A. Olbrich, and B. Ebersberger, Microelectronic Engineering 9, 265-269 (2001).

[28] D. M. Schaadt, E. T. Yu, V. Vaithyanathan, and D. G. Schlom, J. Vac. Sci. Tech (B) 22, 2030-2034 (2004).

[29] Sergei V. Kalinin and D. A. Bonnell, Nano Lett. 4, 555 -560 (2004).

[30] S. Prasertchoung, V. Nagarajan, Z. Ma, R. Ramesh, J. S. Cross, and M. Tsukada, Appl. Phys. Lett. 84, 3130-3132 (2004).

[31] J. A. Christman, J. R. R. Woolcott, A. I. Kingon, and R. J. Nemanich, Appl. Phys. Lett 73, 3851-53 (1998).

[32] V. Nagarajan, A. Roytburd, A. Stanishevsky, S. Prasertchoung, T. Zhao, L. Chen, J. Melngailis, O. Auciello, and R. Ramesh, Nature: Materials 2, 43-47 (2003).

[33] A. T. J. van Helvoort, O. Dahl, B. G. Soleim, R. Holmestad, and T. Tybell, Appl. Phys. Lett. 86, 092907 (2005).

[34] S. Stemmer, S. K. Streiffer, F. Ernst, and M. Ruhle, Philosophical Magazine A-Phys. Of Condensed Matter Structure Defects And Mechanical Properties 71, 713-724 (1995).

[35] R. E. Cohen, Nature 358, 136 (1992).

[36] J. Junquera, Unpublished.

[37] M. E. Lines and A. M. Glass, *Principles and Applications of Ferroelectrics and Related Materials* (Oxford University Press, Oxford, 1977).

[38] W. L. Zhong, B. D. Qu, P. L. Zhang, and Y. G. Wang, Phys. Rev. B 50, 12375-12380 (1994).

[39] A. K. Tagantsev, V. O. Sherman, K. F. Astafiev, J. Venkatech, and N. Setter, J. of Electroceramics 11, 5-66 (2003).

[40] A. K. Tagantsev, M. Landivar, E. Colla, and N. Setter, J. of Appl. Phys. 78, 2623 (1995).

[41] V.Nagarajan, S. Zhong, and S. P. Alpay, Unpublished.

[42] W. L. Warren, G. E. Pike, K. Vanheusden, D. Dimos, B. A. Tuttle, and J. Robertson, J. of Appl. Phys. 79, 9250 (1996).

[43] W. L. Warren, D. Dimos, B. A. Tuttle, G. E. Pike, R. W. Schwartz, P. J. Clews, and D. C. McIntyre, J. of Appl. Phys. 77, 6695 (1995).

[44] W. L. Warren, D. Dimos, B. A. Tuttle, R. D. Nasby, and G. E. Pike, Appl. Phys. Lett. 65, 1018 (1994).

[45] G. Catalan, M. H. Corbett, R. M. Bowman, and J. M. Gregg, Appl. Phys. Lett. 74, 3035 (1999).

[46] U. V. Waghmare and K. M. Rabe, Phys. Rev. B 55, 6161 (1997).

[47] M. G. Stachiotti, Appl. Phys. Lett 84, 251-253 (2004).

[48] I. Kornev, H. Fu, and L. Bellaiche, Phys. Rev. Lett 93, 1961041-4 (2004).

[49] N. A. Pertsev, A. G. Zembilgotov, and A. K. Tagantsev, Phys. Rev. Lett 80, 1988 (1998).

[50] K. J. Choi, M. Biegalski, Y. L. Li, A. Sharan, J. Schubert, R. Uecker, P. Reiche, Y. B. Chen, X. Q. Pan, V. Gopalan, L.-Q. Chen, D. G. Schlom, and C. B. Eom, Science 306, 1005 (2004).

[51] O. Diéguez, S. Tinte, A. Antons, C. Bungaro, J. B. Neaton, K. M. Rabe, and D. Vanderbilt, Phys. Rev. B 69, 212101 (2004).

Figure Captions:

Fig 1(a): High-resolution lattice image of the PZT film grown on SRO/STO. The film is 14 unit cells thick. The image shows a sharp and coherent interface between the ferroelectric and bottom electrode. Fig 1(b) *c* and *a* axis lattice parameter as a function of layer. The lattice parameter of $SrTiO_3$ (3.905Å) was used to calibrate the values. Fig 1(c) Lattice tetragonality for each layer.

Fig 2 :(a) Synchrotron x-ray (002) scan for the 50Å thick film. The peak position of (002)PZT, (200)SRO and STO are labeled. (b) HKL scan around (102) peak of the 50Å thick film. (c) Tetragonality measured as a function of film thickness. For films below 200 Å thick a 1% increase in the tetragonality is observed due to in-plane compression.

Fig 3: DC-AFM images (a)-(d): The images are a 1X1 μm^2 scan of the 50 Å PZT/SRO/STO sample. The sample has low leakage, characterized by the absence of bright regions (refer to the legend on the right for each image). Only on the application of high fields (2.4 MV/cm) do white , highly conductive regions appear as seen in (d).

Fig 4 Switchable polarization as a function of film thickness. Fig 4(a) shows the switching transients (ΔP) as a function of film thickness for a pulse width of 2 μsec and applied field of 2 MV/cm. A clear decrease in the signal is observed as a function of decreasing thickness, thus suggesting a decrease in switchable polarization. The inset shows the switching transient for a 50Å thick film. (b) ΔP as a function of film thickness calculated by integration of the switching transients. As the film thickness is decreases,

the magnitude of switchable polarization decreases; thus the films, in contrast to the structural measurements, show a clear size effect in the polarization measurements. (c) Switched polarization as a function of applied field for 5 thicknesses. The thinner films show significantly high switching field and low switched polarization.

Fig 5(a) Out-of-plane piezoelectric constant d_{33} loops for 5 different thickness. It too shows a clear decrease with decreasing thickness; although the coercive voltage increases. (b) d_{33} as a function of film thickness. The trend shown by the d_{33} is similar to the polarization; an unexpected decrease as a function of decreasing thickness. In the case of a real size effect, the d_{33} is expected to increase with decreasing size.

Fig. 6: Thickness dependence of the normal average polarization P, the tetragonality c/a, and the out-of-plane piezoelectric constant d_{33} at room temperature. Values of these quantities at the bulk level are represented by dashed lines for the unstrained configuration, and dotted lines for a geometry under the strain imposed by the substrate. The evolution of the domain structure, from a monodomain configuration at large thicknesses, where the depolarization field E_d is small, to a 180º stripe domains to minimize the energy associated with E_d is represented in the inset. Standard deviation distributions, obtained from averaging over different number of Monte Carlo steps in many simulations, starting with different seeds for the random number generator, are indicated by error bars.

Fig. 7: Local mode displacements of the cells situated in a transverse cut of the film at different thickness: 350 Å (a), 150 Å(b), and 60 Å (c). The arrows give the direction of the displacement projected on a yz plane, where z is the normal direction to the interface, and the arrows length indicates the projected magnitudes. A sharp monodomain-polydomain phase transition is observed at a thickness around 150 Å. Above this critical thickness (panel a), the local mode is reduced, and even locally reversed by the effect of the residual depolarization field. Below the critical thickness, domains of opposite polarization nucleate and grow with decreasing thickness till a 50/50 configuration, with no net polarization, is formed.

Fig 8 : Thickness dependence of the normal average polarization under the effect of an external applied field of 3MV/cm at room temperature. Even at such high fields, the 180º domains remain pinned, thus resulting in a reduced average polarization. The bulk strained value in zero field (dashed line) is represented for comparison. The error bars have the same meaning as in Fig. 3.

Fig 9: Piezoresponse Force Microscopy (PFM) image for the 150Å and 50Å thick films. Fig 9(a) is the PFM image after application of +5 and -5 bias to inner 3 μm^2 and 1 μm^2 regions respectively. Fig (b) is the profile AA' of (a). (c) and (d) are respective PFM and profiles for the 50Å thick film. The contrast scales are the same for both images.

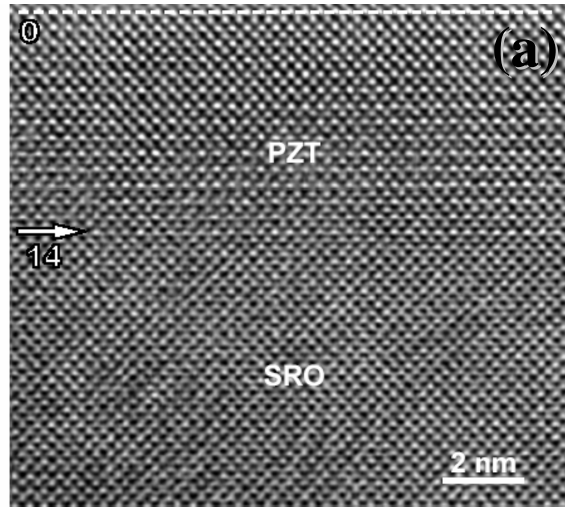

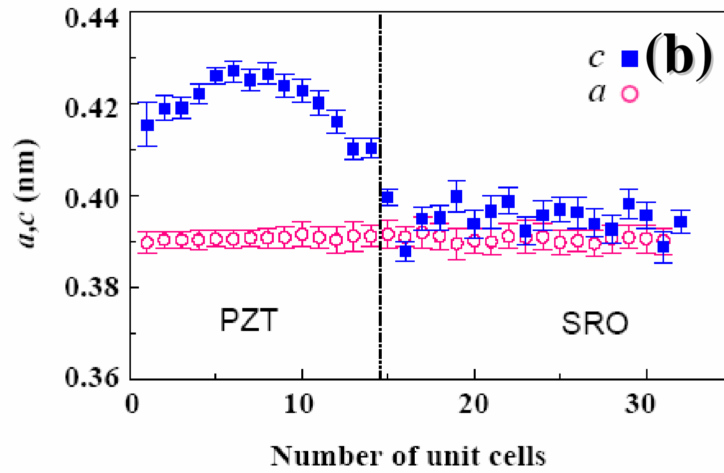

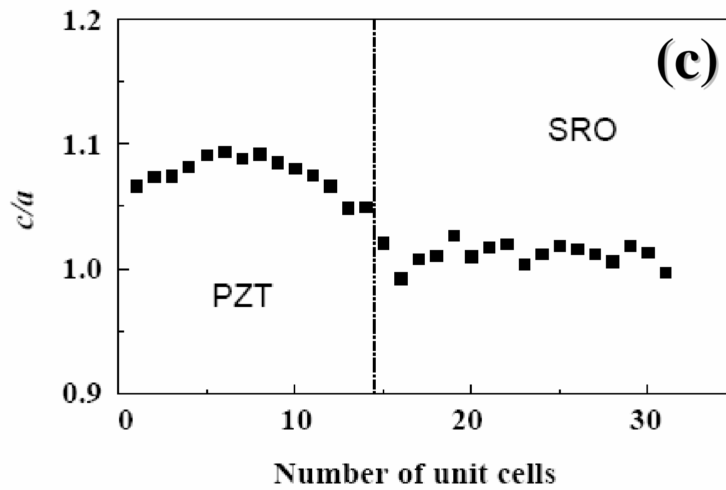

Figure 1

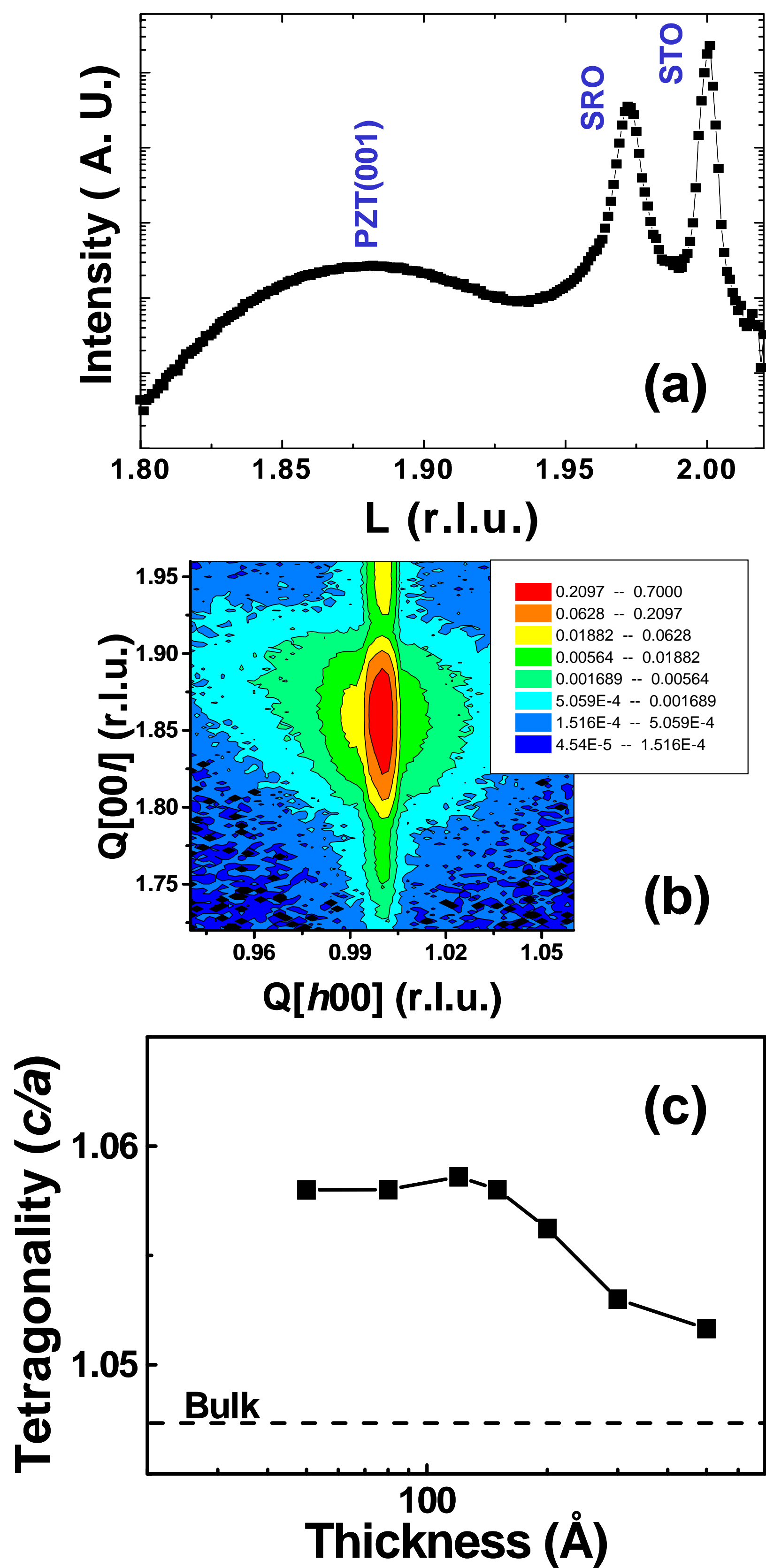

Figure 2

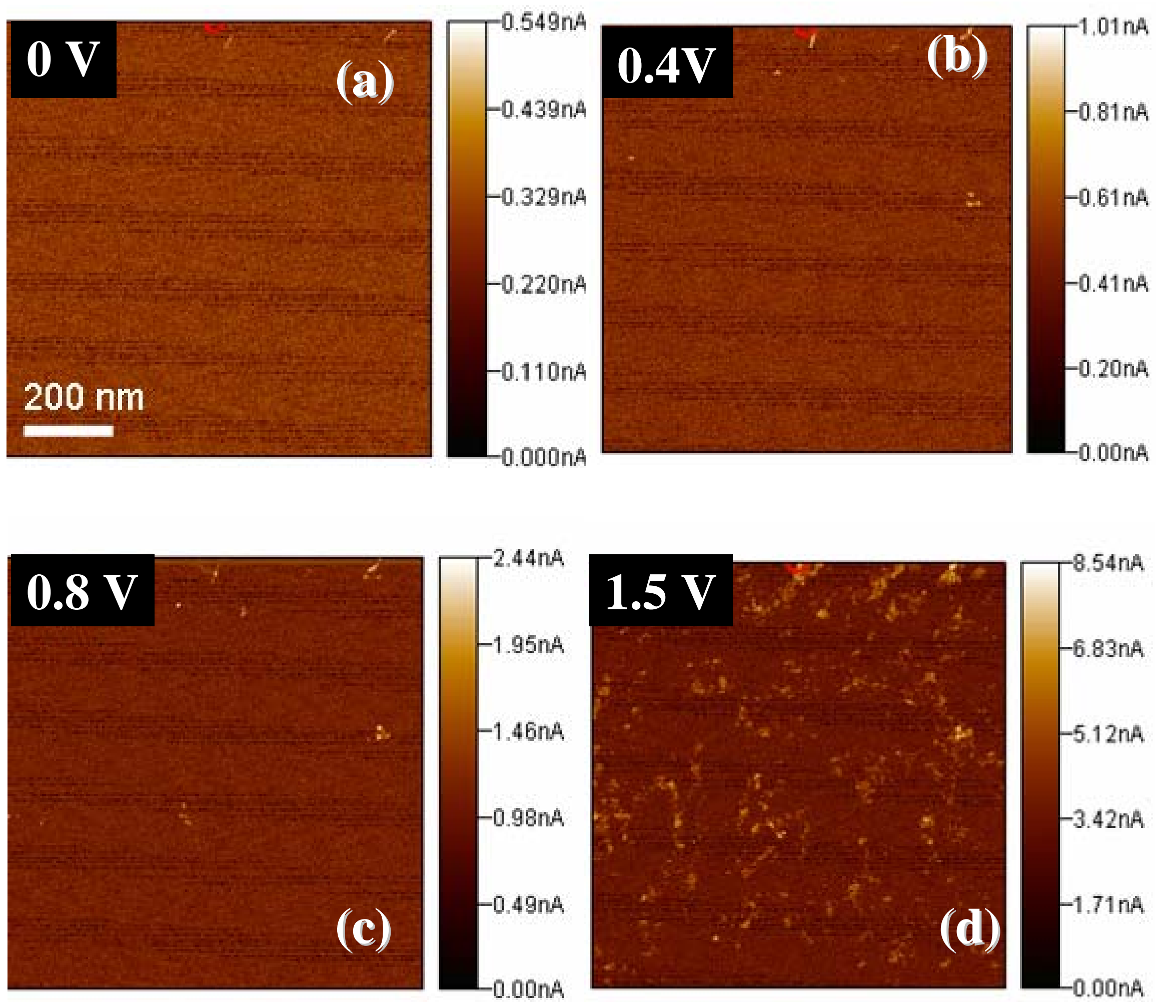

Figure 3

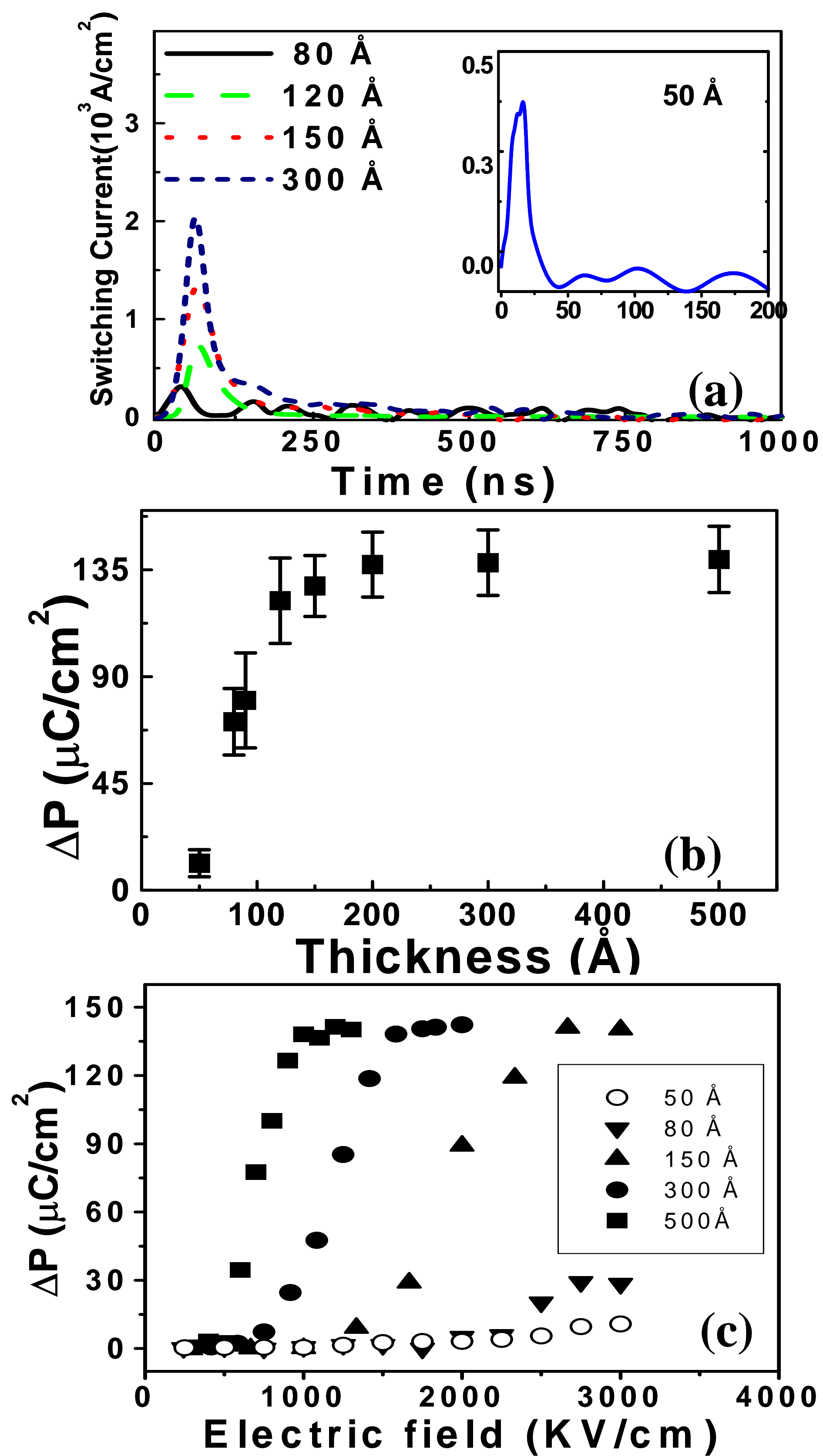

Figure 4

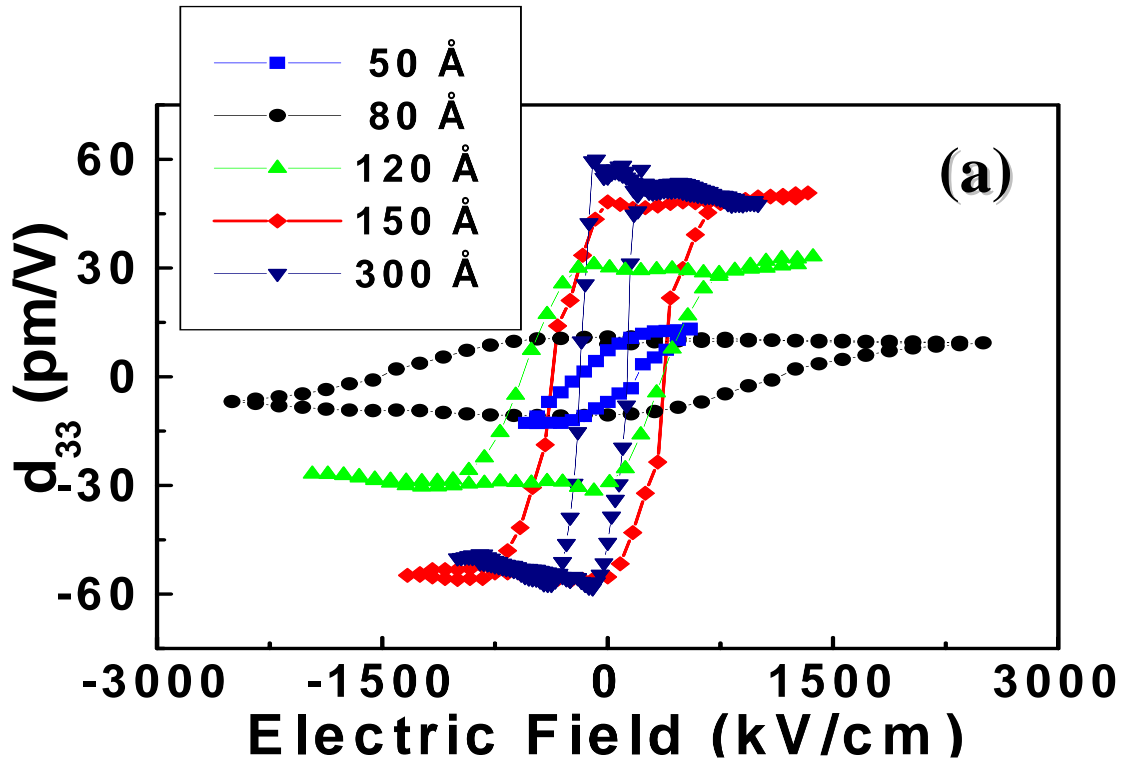

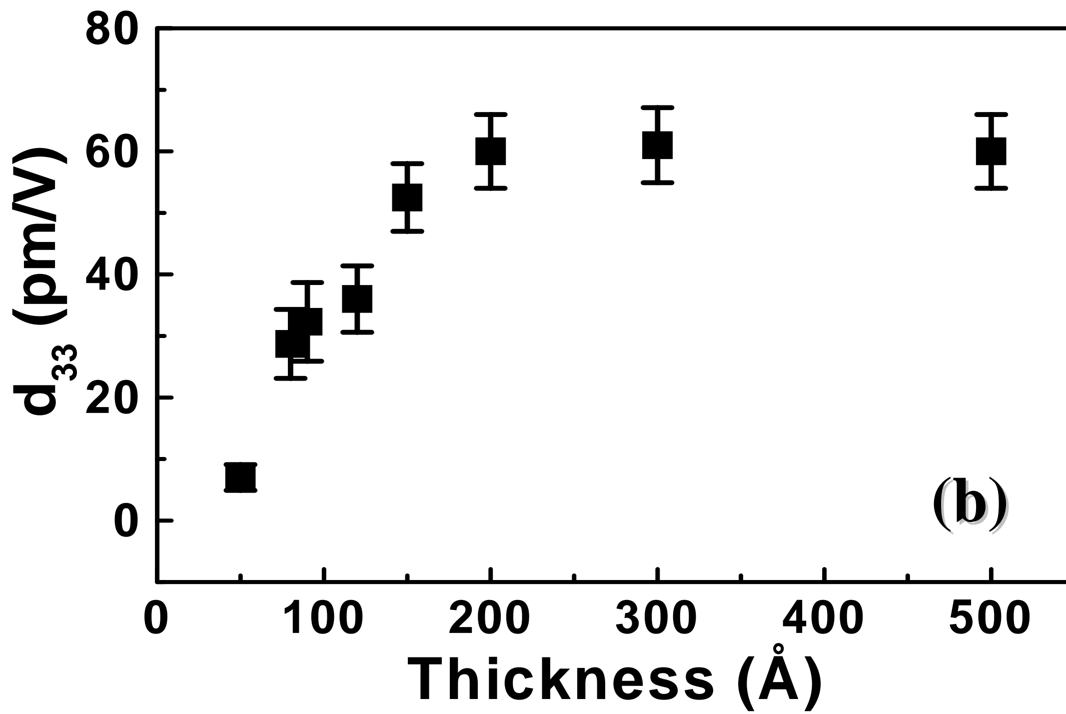

Figure 5

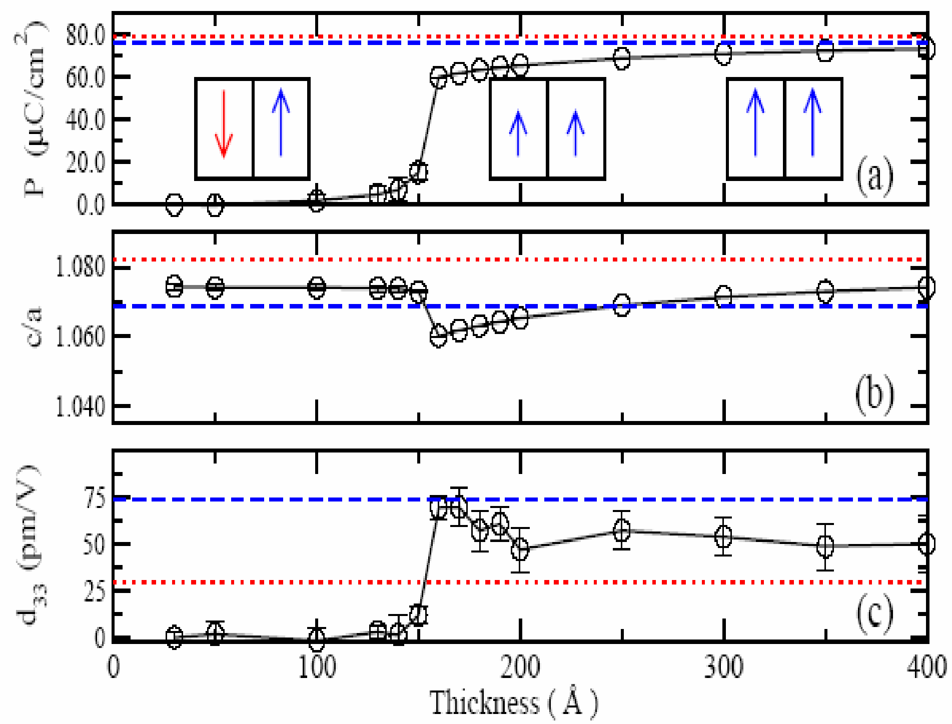

Figure 6

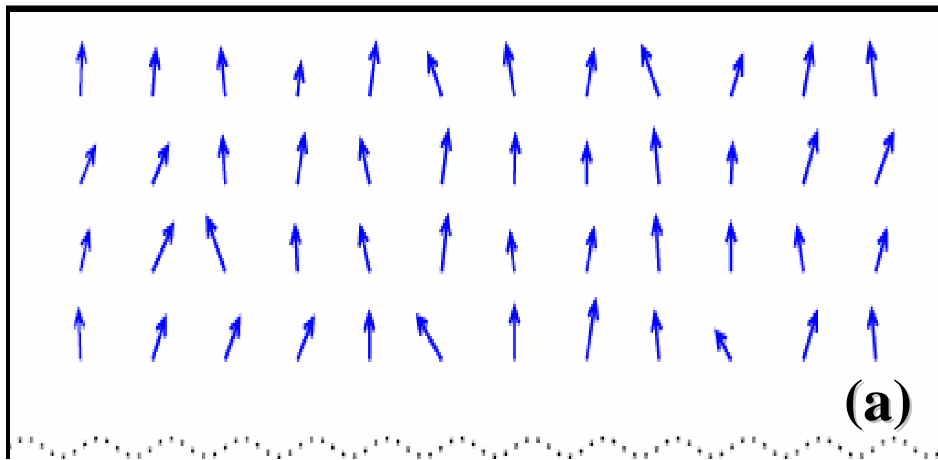

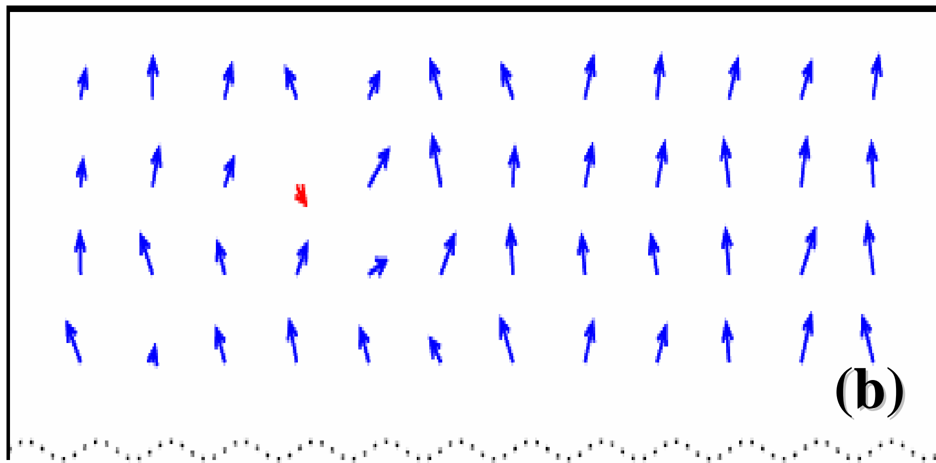

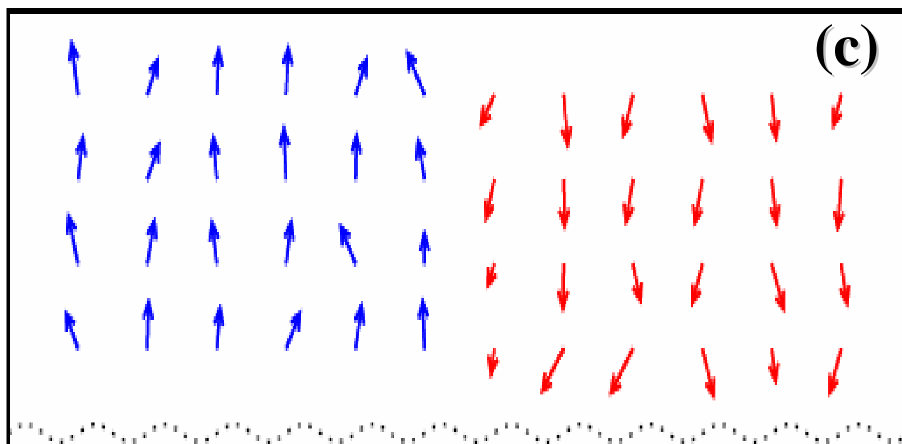

Figure 7

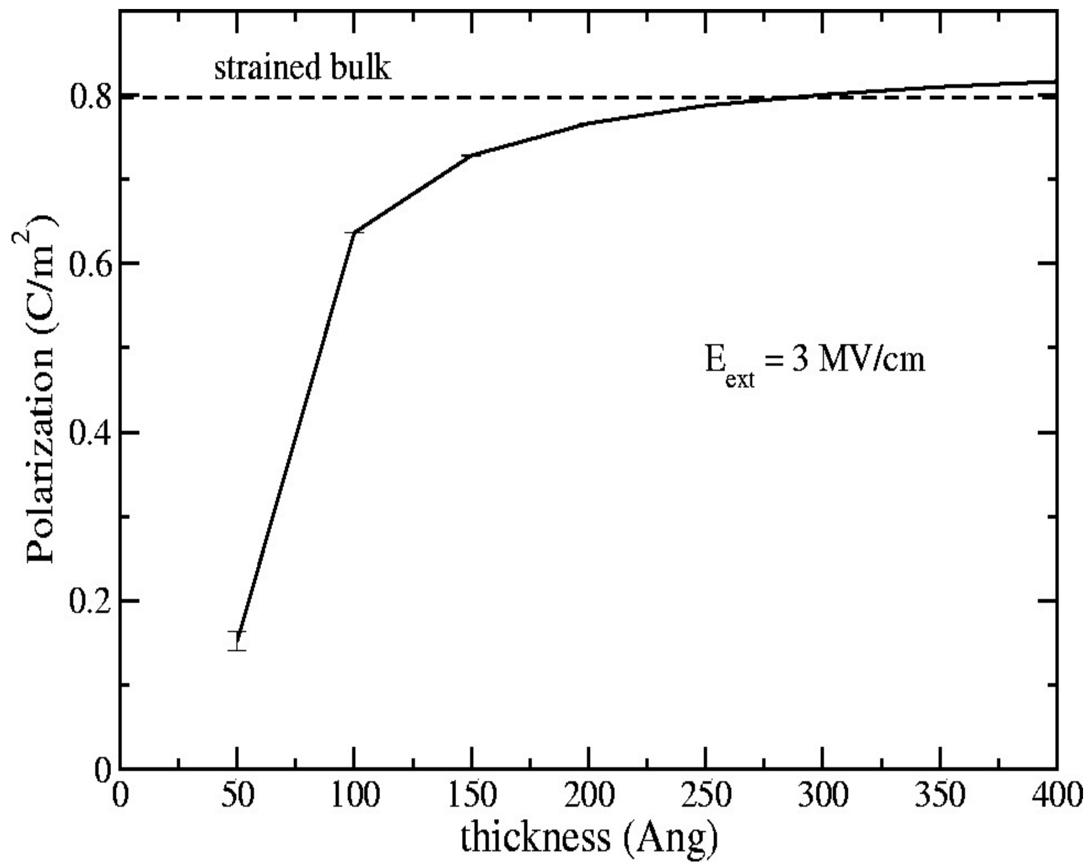

Figure 8

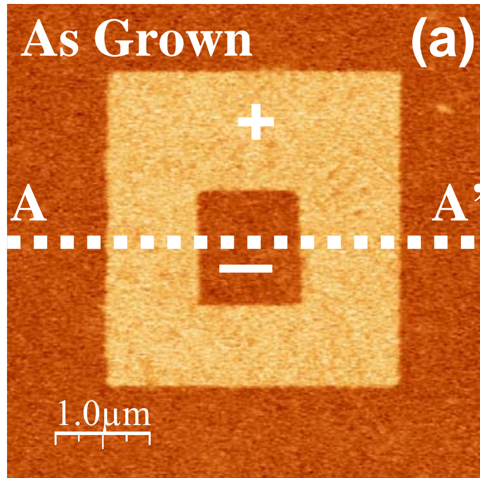

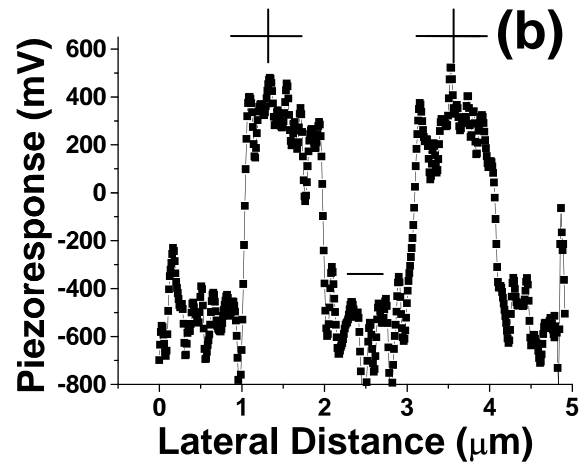

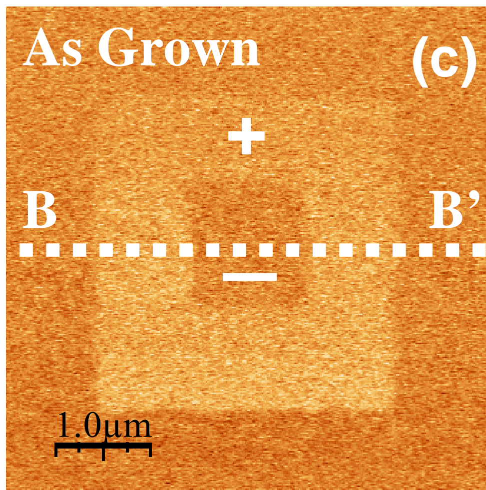

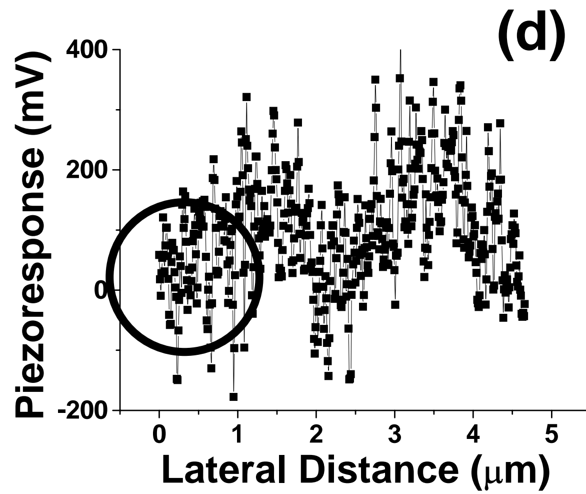

Figure 9